**Conference on New Frontiers in Scaling Quantum: from Materials and Hardware to Architectures and Components | (SMR 3916)**

15 Jan 2024 - 19 Jan 2024
ICTP, Trieste, Italy

**P01 - ARNOLD Georg**

All-optical superconducting qubit readout

**P02 - BABLA Harshvardhan Kiran**

Fault-Tolerant Fusion-Based Quantum Computing with the 4-Legged Cat Code

**P03 - BERKE Christoph**

A many-body perspective on transmon-based quantum computers

**P04 - BOUAFIA Zakaria**

Effects of thermal noise on quantum correlations and interferometric power in a graphene layer system with a scattering process

**P05 - CORAIOLA Marco**

Large spin splitting of Andreev levels in three-terminal Josephson junctions

**P06 - DHUNDHWAL Ritika**

Material losses characterization in superconducting resonators based on $\alpha$ and $\beta$ Tantalum

**P07 - FARYAD Muhammad**

Noise analysis of Grover and phase estimation algorithms implemented as quantum singular value transformations for small number of noisy qubits

**P08 - FRAU Martina**

Quanifying magic (and its relation to entanglement) beyond qubits: the case of S=1 chains

**P09 - GHARIBAAN Rebecca**

Towards microwave experiments in III-V 2DEGs

**P10 - GUO Shaojun**

Experimental quantum computational chemistry with optimised unitary coupled cluster ansatz

**P11 - HU Yong**

Skyrmion-Based Magnetic Recording and Storage

**P12 - JOVEN NORIEGA Kevin Jofroit Jofroit**

Quantum Circuit Optimization based on mid-circuit Entanglement

**P13 - KAPOOR Lucky**

Exploring fluxon tunneling dynamics in the IST qubit

**P14 - KHORRAMSHAHI Mahya**

High-impedance resonators based on granular aluminum

**P15 - KHVALYUK Anton**

Near-power-law temperature dependence of the superfluid stiffness in strongly disordered superconductors

**P16 - KOGAN Evgeni**

Poor man's scaling and Lie algebras

**P17 - LEVIN Andrei**

Effect of superconductivity on non-uniform magnetization in dirty SF junctions

**P18 - LUNKIN Aleksey**

The butterfly effect in a Sachdev-Ye-Kitaev quantum dot system

**P19 - OSIN Aleksandr Sergeevich**

Anomalous Josephson effect in superconducting multilayers

**P20 - POBOIKO Ihor**

Theory of free fermions under random projective measurements

**P21 - RAJPOOT Garima**

Quantum error correction beyond the toric code

**P22 - SAFONOVA Elizaveta**

Intensity statistics inside an open wave-chaotic cavity with broken time-reversal invariance

**P23 - SEIDA Chaibata**

Two-way quantum teleportation under correlated noise

**P24 - SETIAWAN Iwan**

Fast-forward generation of non-equilibrium steady states of a charged particle under the magnetic field

**P25 - SHI Pan**

Multiplexed control scheme for scalable superconducting quantum processor

**P26 - TARABUNGA Poetri Sonya**

Many-body magic via Pauli-Markov chains

**P27 - TIRRITO Emanuele**

Quantifying non-stabilizerness through entanglement spectrum flatness

**P28 - VAN THIEL Thierry Christiaan**

Optical readout of a superconducting qubit using a piezo-optomechanical transducer

**P29 - WANG Ruixia**

Suppressing spurious transitions using spectrally balanced derivative pulse

**P30 - YE Yangsen**

Logical Magic State Preparation with Fidelity beyond the Distillation Threshold on a Superconducting Quantum Processor

**P31 - ZAPATA GONZALEZ Nicolas**

Near quantum-limited amplification up to 1 T using grAl resonators

# All-optical superconducting qubit readout

**Georg Arnold** [1], **Thomas Werner** [1], **Rishabh Sahu, Lucky N. Kapoor, Liu Qiu, and Johannes M. Fink** [2]

[1] *Institute of Science and Technology Austria, Am Campus 1, 3400 Klosterneuburg, Austria*

The rapid development of superconducting quantum hardware is expected to run into significant I/O restrictions due to the need for large-scale error-correction in a cryogenic environment [1]. Classical data centers rely on fiber-optic interconnects to remove similar networking bottlenecks. In the same spirit, ultra-cold electro-optic links have been proposed and used to generate qubit control signals [2], or to replace cryogenic readout electronics. So far, the latter suffered from either low efficiency [3], low bandwidth and the need for additional microwave drives [4], or breaking of Cooper pairs and qubit states [5]. Here, we present a radio-over-fiber qubit readout that does not require any active or passive cryogenic microwave equipment. We demonstrate all-optical single-shot readout by means of the Jaynes-Cummings nonlinearity [6] in a circulator-free readout scheme. Specifically, we replace the complete cryogenic microwave input and output by an optical fiber and a single electro-optic transducer operated at mK temperatures. The latter is used simultaneously for demodulation of the input probing the qubit state as well as for modulation of the telecom light by means of the reflected microwave tone carrying information of the qubit state. Even though the active optical heat load in the electro-optic link prevents substantial scaling-up of this first-generation implementation, the fundamental limit of this minimalistic readout is orders of magnitudes below standard microwave readouts or other dissipative approaches [2]. Importantly – we do not observe any direct impact of the laser light on the qubit performance, as verified with high-fidelity quantum-non-demolition measurements. This compatibility between superconducting circuits and light is not only a prerequisite to establish modular quantum networks [7], it is also relevant for classical superconducting logic. The presented work furthermore showcases the potential of electro-optic radiometry in harsh environments.

[1] S. Bravyi, O. Dial, J. M. Gambetta, D. Gil, and Z. Nazario, J. of App. Phy. **132**, 60902 (2022)

[2] F. Lecocq, F. Quinlan, K. Cicak, J. Aumentado, S. A. Diddams, and J. D. Teufel, Nature **591**, 575 (2021).

[3] A. Youssefi, I. Shomroni, Y. J. Joshi, N. R. Bernier, A. Lukashchuk, P. Uhrich, L. Qiu, and T. J. Kippenberg, Nature Electronics **4**, 326 (2021)

[4] R. D. Delaney, M. D. Urmey, S. Mittal, B. M. Brubaker, J. M. Kindem, P. S. Burns, C. A. Regal, and K. W. Lehnert, Nature **606**, 489 (2022).

[5] M. Mirhosseini, A. Sipahigil, M. Kalaee, and O. Painter, Nature **588**, 599 (2020).

[6] M. D. Reed, L. DiCarlo, B. R. Johnson, L. Sun, D. I. Schuster, L. Frunzio, and R. J. Schoelkopf, Phys. Rev. Lett. **105**, 173601 (2010).

[7] J. Ang, G. Carini, Y. Chen, I. Chuang, M. A. DeMarco, S. E. Economou, A. Eickbusch, A. Faraon, K.-M. Fu, S. M. Girvin, M. Hatridge, A. Houck, P. Hilaire, K. Kr sulich, A. Li, C. Liu, Y. Liu, M. Martonosi, D. C. McKay, J. Misewich, M. Ritter, R. J. Schoelkopf, S. A. Stein, S. Sussman, H. X. Tang, W. Tang, T. Tomesh, N. M. Tubman, C. Wang, N. Wiebe, Y.-X. Yao, D. C. Yost, and Y. Zhou, Architectures for Multinode Superconducting Quantum Computers (2022), arXiv:2212.06167.

# Fault-Tolerant Fusion-Based Quantum Computing with the 4-Legged Cat Code

**Harshvardhan K. Babla** [1,2] , **James D. Teoh** [1,2] , **Jahan Claes** [1,2],

**Robert J. Schoelkopf** [1,2] , **Shruti Puri** [1,2]

[1] *Departments of Applied Physics and Physics, Yale University, New Haven, CT, USA*
[2] *Yale Quantum Institute, Yale University, New Haven, CT, USA*

With its ability to correct for single-photon loss, the 4-legged cat code stands out as a promising bosonic quantum memory, becoming the first code to surpass the QEC breakeven point [1]. We extend its capabilities with a universal set of operations composed of destructive Bell measurements and entangled resource state generation. These operations are efficiently implemented using standard circuit QED tools: inter-cavity beam-splitter coupling, cavity displacements, and cavity-transmon dispersive coupling, and transmon drives. Notably, our proposal circumvents common experimental challenges in circuit QED, such as: parameter matching, Hamiltonian engineering, and undesired non-linearities in the storage cavity. Additionally, analytics and pulse-level simulations demonstrate that these operations are, at worst, second-order sensitive to both photon loss in the storage cavity and decoherence in the transmons. The proposed universal set of operations is particularly suited for fusion-based fault-tolerant quantum computation with the XZZX cluster state. The inherent first-order robustness promises a suppression of physical qubit error rates beyond what is expected from unencoded physical qubits.

[1] Ofek et. al. Nature 536, 441–445 (2016)

# A many-body perspective on transmon-based quantum computers

Christoph Berke[1] and Simon Trebst[2]

[1]Institut for Theoretical Physics, University of Cologne

We fuse the disparate fields of quantum processor engineering and many-body localization / quantum chaos. From a many-body perspective, transmon architectures are synthetic systems of interacting and disordered nonlinear quantum oscillators. We analyze small instances of transmon arrays in exact diagonalization studies and scrutinize whether the disorder in the Josephson energies found in prevalent processor architectures can protect the transmon quantum computer (or rather quantum memory) from the destabilizing effects of the inter-qubit coupling [1]. Our studies are further supplemented by classical simulations. We demonstrate that those lead to similar stability metrics as the quantum simulations (classical Lyapunov exponents vs. quantum wave function participation ratios) in systems with O(10) transmons. The crucial point of the classical simulation is that it can be pushed to large systems comprising up to thousands of qubits. We find a systematic increase of Lyapunov exponents in system size, suggesting that larger layouts require added efforts in information protection [2]. Furthermore, we examine to what extent fast gate operations, which involve the transient population of states outside the computational subspace, can be affected by chaotic fluctuations. We consider the eigenphases and -states of the time evolution operators describing a universal gate set, and analyze them by the many-body methodology. We observe that fast entangling gates, operating at speeds close to the so-called quantum speed limit, contain transient regimes where the dynamics indeed becomes partially chaotic. We find that for these gates even small variations of Hamiltonian or control parameters lead to large gate errors [3].

[1] Christoph Berke, Evangelos Varvelis, Simon Trebst, Alexander Altland, David P. DiVincenzo, Transmon platform for quantum computers challenged by chaotic fluctuations Nature Communications 13, 2495 (2022)
[2] Simon-Dominik Börner, Christoph Berke, David P. DiVincenzo, Simon Trebst, Alexander Altland, Classical Chaos in Quantum Computers arXiv:2304:14435 (2023).
[3] Daniel Basilewitsch, Simon-Dominik Börner, Christoph Berke, Alexander Altland, Simon Trebst, Christiane P. Koch, Chaotic fluctuations in a universal set of transmon qubit gates arXiv:2311.14592 (2023).

# Effects of thermal noise on quantum correlations and interferometric power in a graphene layer system with a scattering process

**Z. Bouafia**[1] **and M. Mansour**[1]

[1]*Laboratory of High Energy Physics and Condensed Matter, Department of Physics,*
*Faculty of Sciences of Aïn Chock, Hassan II University,*
*Casablanca, Morocco*

Cutting-edge quantum processing technology is currently exploring the remarkable electronic properties of graphene layers, such as their high mobility and thermal conductivity. Our research is dedicated to investigating the behavior of quantum resources within a graphene layer system with a scattering process, specifically focusing on quantum interferometric power (QIP) and quantum correlations, while taking into account the influence of thermal noise. To quantify these correlations, we employ measures like local quantum uncertainty (LQU) and logarithmic negativity (LN). We examine how factors like temperature, inter-valley scattering process strength, and other system parameters affect both QIP and quantum correlations. Our results reveal that higher temperatures lead to a reduction in QIP and non-classical correlations within graphene layers. Moreover, it is noteworthy that QIP and LQU respond similarly to changes in temperature, whereas LN is more sensitive to these variations. By optimizing system parameters such as band parameter, wavenumber operators and scattering process strength, we can mitigate the impact of thermal noise and enhance the quantum advantages of graphene-based quantum processing.

[1]  Z. Bouafia and M. Mansour, Laser Phys. Lett. **20**, 125204 (2023).

# Large spin splitting of Andreev levels in three-terminal Josephson junctions

**Marco Coraiola[1], Daniel Z. Haxell[1], Deividas Sabonis[1], Manuel Hinderling[1], Sofieke C. ten Kate[1], Erik Cheah[2], Filip Krizek[2], Rüdiger Schott[2], Werner Wegscheider[2], and Fabrizio Nichele[1]**

*[1] IBM Research Europe – Zurich, 8803 Rüschlikon, Switzerland*
*[2] Laboratory for Solid State Physics, ETH Zürich, 8093 Zürich, Switzerland*

Harnessing spin and parity degrees of freedom is of fundamental importance for the realization of emergent quantum devices. Nanostructures realized in superconductor-semiconductor hybrid materials offer novel and yet unexplored routes for encoding and manipulating qubit states.

We report spectroscopic measurements of the two-dimensional band structure formed by Andreev bound states in a phase-controlled hybrid three-terminal Josephson junction [1, 2]. Andreev bands reveal breaking of the spin degeneracy, with level splitting in excess of 9 GHz, and zero-energy crossings associated to ground state fermion parity transitions, in agreement with theoretical predictions [3]. Both effects occur without the need for external magnetic fields or sizable charging energies and are tuned locally by controlling superconducting phase differences.

Our results highlight the potential of hybrid multiterminal devices in engineering quantum states. Specifically, the large splitting between spin-resolved Andreev levels opens the door for next-generation superconducting spin qubits [4, 5].

[1] M. Coraiola et al., Nat. Comm. **14**, 6784 (2023)
[2] M. Coraiola et al., arXiv:2307.06715 (2023)
[3] B. van Heck, S. Mi, A. R. Akhmerov, Phys. Rev. B **90**, 155450 (2014)
[4] M. Hays et al., Science **373**, 440-443 (2021)
[5] M. Pita-Vidal et al., Nat. Phys. **19**, 1110-1115 (2023)

# Material losses characterization in superconducting resonators based on $\alpha$ and $\beta$ Tantalum

**Ritika Dhundhwal**[1], Haoran Duan[2], Lucas Brauch[1], Soroush Arabi[1], Qili Li[3], Sudip Pal[6], Jose Palomo[5], Dirk Fuchs[1], Alexander Welle[4], Mark Scheffler[6], Zaki Leghtas[5], Jasmin Aghassi-Hagmann[2], Christian Kübel[2], Wulf Wulfhekel[1], Ioan M. Pop[1,3,6] and Thomas Reisinger[1]

[1]*Institut für Quantenmaterialien und Technologien, Karlsruher Institut für Technologie*
[2]*Institute of Nano Technology, Karlsruher Institut für Technologie*
[3]*Physikalisches Institut, Karlsruher Institut für Technologie*
[4]*Institut für Funktionelle Grenzflächen, Karlsruher Institut für Technologie*
[5]*École Normale Supérieure, Paris*
[6]*Unversity of Stuttgart, Stuttgart*

Implementation of tantalum as a new material platform in transmon qubit has shown promising results with coherence time exceeding 0.3 ms[1]. To understand the underlying cause for record breaking coherence times, the main focus has been on use of alpha phase tantalum to achieve high quality qubits and resonators whereas the beta phase remains largely unexplored. In this work, we compare internal quality factor in lumped element resonators as a function of photon number and temperature. We use various material characterization tools to investigate surface and bulk properties of tantalum. Further, we vary the energy participation ratio in tantalum metal-substrate and metal-air interfaces to estimate the loss tangent and get insight into dominant loss mechanism.

[1] Place, A.P.M., Rodgers, L.V.H., Mundada, P. et al., Nat Commun **12**, 1779 (2021).

# Noise analysis of Grover and phase estimation algorithms implemented as quantum singular value transformations for small number of noisy qubits

**Muhammad Abdullah Ijaz**[1] **and Muhammad Faryad**[1,*]

[1]Department of Physics, Lahore University of Management Sciences, Lahore, 54792, Pakistan.
[*]muhammad.faryad@lums.edu.pk

## ABSTRACT

Quantum singular value transformation (QSVT) algorithm is a general framework to implement most of the known algorithms and provides a way forward for designing new algorithms. In the present work, the impact of noise on the QSVT algorithm is examined for bit flip, phase flip, bit-phase flip, and depolarizing noise models for a small number of qubits. The small number of noisy qubits approximates the currently available noisy quantum computers. For simulation results, the QSVT implementation of the Grover search and quantum phase estimation (QPE) algorithms is considered. These algorithms are among the basic quantum algorithms and form the building blocks of various applications of quantum algorithms. The results showed that the QSVT implementation of the Grover search and QPE algorithms has consistently worse dependence upon noise than the original implementation of these algorithms for all four noise models.

## Introduction

Grover search and quantum phase estimation (QPE) are two major quantum algorithms that act as building blocks for many other quantum algorithms[1]. Both of these algorithms provide distinct speed-up over their classical counterparts. Recently, a unifying quantum algorithm, namely, the quantum singular value transformation (QSVT) algorithm was discovered that generalizes many known algorithms including Grover search and QPE[2].

The QSVT framework was essentially anticipated earlier as quantum signal processing and block encoding[3–6] before its consolidation[2] with the specializations to Grover search, phase estimation, Hamiltonian simulation, and HHL following later[7]. The QSVT allows for the implementation of arbitrary polynomials[2,8,9], which need only be sufficiently well-behaved. Moreover, since QSVT uses singular value decomposition, non-square and non-unitary operations can also be implemented in the QSVT circuit. The advantages of the QSVT regime are undeniable as we can use it to implement a wide range of simple algorithms like the Grover search and complex algorithms like the feedback-dependent phase estimation. Not only do the QSVT implementations match the complexity advantage of the non-QSVT Grover search and phase estimation algorithm in the limit of large qubits, but the search problem can also be adjusted to avoid the convergence problem, and the phase estimation in the QSVT framework implements $\hat{U}_p^{2^j}$ more reliably[7].

In the limit of large qubits, both the original quantum algorithms and their QSVT generalizations provide similar algorithmic complexity. However, in the limit of small number of qubits, the overhead of QSVT algorithm demands higher gate count for basic quantum algorithms like Grover search and QPE than the original implementations of these algorithms. This is important because of the small and noisy quantum computers of today that are very sensitive to the number of gates in a given circuit[10]. Therefore, we set out to investigate the impact of various noise models on the implementation of Grover and QPE algorithms if implemented using QSVT in the limit of small number of qubits. For this purpose, the salient features relevant to our work of the QSVT, Grover, and QPE algorithms are discussed in Sec. The Algorithms. The simulation results with various noise models are presented in Sec. Results and concluding remarks are presented in Sec. Discussion.

All the operators are decorated with a hat, vectors are represented with uppercase Greek alphabets and the quantum states are represented using the usual Dirac notations.

## The Algorithms

### Quantum Singular Value Transformation:

The basis of the QSVT algorithm is the singular value transformation, which can decompose any arbitrary matrix $\hat{A}$ as

$$\hat{A} = \sum_{k=1}^{r} \sigma_k \left| u_k \right\rangle \left\langle v_k \right|$$ (1)

by decomposing the matrix as $\hat{A} = \hat{P}'\hat{U}\hat{P}$, where $\hat{P}$ and $\hat{P}'$ are projection operators spanning the vector spaces $\left| u_k \right\rangle$ and $\left| v_k \right\rangle$, respectively, and the singular values $\sigma_k$ being non-negative and real. Hence we can block encode the matrix $\hat{A}$ as[2]

$$\hat{U} = \begin{bmatrix} \hat{A} & \sqrt{I-\hat{A}^2} \\ \sqrt{I-\hat{A}^2} & \hat{A} \end{bmatrix}.$$

Substituting the unitary $\hat{U}$ and projection-controlled phase operators as rotation operators in the quantum signal processing algorithm allows for the construction of unitaries[6]

$$\hat{U}_\Phi = \hat{P}'_{\phi_1}\hat{U} \left[ \prod_{k=1}^{(d-1)/2} \hat{P}_{\phi_{2k}}\hat{U}^\dagger \hat{P}'_{\phi_{2k+1}}\hat{U} \right], \quad d \in \{1,3,5,...\},$$

$$\hat{U}_\Phi = \prod_{k=1}^{d/2} \hat{P}_{\phi_{2k-1}}\hat{U}^\dagger \hat{P}'_{\phi_{2k+1}}\hat{U}, \qquad d \in \{2,4,6,...\},$$

which can implement any polynomial $Poly^{(SV)}(\hat{A})$ on the domain of $\sigma_k \in [-1,1]$ with the rotation parameters $\Phi = (\phi_1, \phi_2, ..., \phi_d)$ and has the properties[11] :

1. $Poly(\hat{A}) \leq d$,

2. $Poly(\hat{A})$ has parity d mod(2),

3. $| Poly(\hat{A}) |^2 + | Poly(\sqrt{I-\hat{A}^2}) |^2 = 1$.

Armed with these operators, we need only determine the polynomial that approximates the problem along with the rotation parameters $\Phi = (\phi_1, \phi_2, ..., \phi_d)$ to construct $\hat{U}_\Phi$[9,11]. For example, the HHL algorithm can be implemented in the QSVT framework to efficiently solve a set of linear equations[12]. Where the polynomial corresponding to HHL is $f(x) = 1/x$ with $\Phi$ determined using algorithms such as Remez-type exchange[8,13].

Within the scope of this paper, we will only focus on the Grove search and phase estimation algorithm and use

$$\Phi = ((1-d)\frac{\pi}{2}, \frac{\pi}{2}, ..., \frac{\pi}{2}),$$ (2)

since both the Grover search and phase estimation algorithms can be represented as $d^{th}$ order Chebyshev polynomials[6,7].

### Grover Search Algorithm

The Grover search algorithm amplifies a state marked by an oracle $\hat{U}_g$ as

$$\hat{U}_g \left| j \right\rangle = (-1)^{\delta_{jm}} \left| j \right\rangle,$$ (3)

where $\delta_{jm}$ is Kronecker delta function. Since we want to amplify the states $\left| m \right\rangle$ from an initial state of uniform superposition $\left| \psi_0 \right\rangle = \hat{H}^{\otimes n} \left| 0 \right\rangle$, the state evolves such that $\hat{U}_\Phi \left| \psi_0 \right\rangle \rightarrow \left| m \right\rangle$, where $\hat{H}$ is the Hadamard transform.

Hence the polynomial takes the form

$$Poly(c_m) = \left\langle m \right| \hat{U}_\Phi \left| \psi_0 \right\rangle,$$ (4)

where $c_m$ is the probability amplitude of $\left| m \right\rangle$ in $\left| \psi_0 \right\rangle$ state. Hence the polynomial has odd parity and the upper-bound: $Poly(1/\sqrt{2^n}) \leq 1$.

The QSVT implementation of the Grover algorithm draws from the fixed point quantum search algorithm, which maintains the complexity advantage of Grover but does not have the convergence problem[14,15]. However, to draw parallels between the
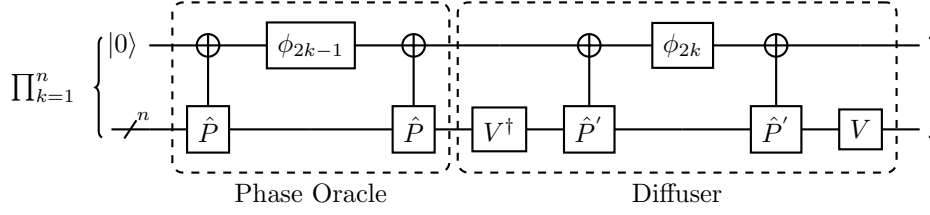
**Figure 1.** The QSVT quantum circuit for Grover search algorithm, composed of the phase rotation gate $\phi$, which takes rotation parameters as input, the unitary $\hat{V} = \hat{H}^{\otimes n}$ operators and the $C_{\hat{P}}NOT$ and $C_{\hat{P}'}NOT$ gates that target the ancilla qubit.

algorithms, the QSVT algorithm implemented here is a simplified Grover circuit such that the non-QSVT oracle and diffuser emerge without losing the unique circuitry of the QSVT framework.

The circuit for the QSVT implementation of the Grover algorithm is shown in Fig. 1. This circuit uses $\mathscr{O}(2^{n/2}(1/\delta))$ queries to the projection-controlled phase operators for both the left and right subspace and the unitary $\hat{V} = \hat{H}^{\otimes n}$ operator along with one ancilla qubit, where $\delta$ is the error tolerance[7]. This leads to probability of success $\geq 1 - \delta$. The marked state used in this implementation corresponds to $|m\rangle = |1\rangle^{\otimes n}$ and the projection operators are $\hat{P} = \hat{I} - |m\rangle\langle m|$ and $\hat{P}' = \hat{I} - |0\rangle\langle 0|$. As mentioned above, the combination of these gates reproduces the non-QSVT Grover search algorithm. The first part of the QSVT Grover iterate, with the phase gate sandwiched between the $C_{\hat{P}}NOT$ gates is equivalent to the oracle $\hat{U}_g$ as it attached a negative phase to the marked state, while the rest acts as the diffuser and reflects the state around the uniform superposition state $|\psi_0\rangle$.

### Quantum Phase Estimation

The QSVT implementation of the QPE algorithm analyzed in this paper is developed in Refs.[7,16], which is a derivative of Kitaev's iterative algorithm and approximates the phase introduced by a unitary $\hat{U}_p$, using a semi-classical feedback process[17,18]. The operator $\hat{U}_p$ introduces the phase $\theta$ to a state $|u\rangle$ and can be represented as,

$$\hat{U}_p |u\rangle = e^{2\pi i \theta} |u\rangle . \tag{5}$$

The QSVT implementation of the QPE is iterative, so in the $l^{th}$ loop, it approximates the $\theta_l$ by encoding the less significant bits: $\theta' = \theta_{l+1}, \theta_{l+2}...\theta_n$. So, the total phase measured after all iterations is found as

$$\theta' = \sum_{l=1}^{n} \frac{\theta_l}{2^l} . \tag{6}$$

The $l^{th}$ iterative component of the QSVT quantum phase estimation algorithm is shown in Fig. 2 which uses

$$\hat{W}_j(\theta') = \frac{1}{2} \begin{bmatrix} \hat{I} + e^{-2\pi i \theta'} \hat{U}_p^{2^j} & \hat{I} - e^{-2\pi i \theta'} \hat{U}_p^{2^j} \\ \hat{I} - e^{-2\pi i \theta'} \hat{U}_p^{2^j} & \hat{I} + e^{-2\pi i \theta'} \hat{U}_p^{2^j} \end{bmatrix} .$$

to estimate $\theta_l$.

This circuit corresponds to the polynomial approximation of the sign function, having an even parity and an upper bound of magnitude 1[7]. Furthermore, it makes $\mathscr{O}(n log(n/\delta))$ queries to the operator $\hat{W}_j$, and the projection controlled phase operators $C_{\hat{P}'}NOT$ where $\hat{P} = \hat{P}' = |0\rangle\langle 0| \otimes \hat{I}$. On the last iteration the circuit outputs $\theta'$, with the error

$$|\theta - \theta'| < \frac{1}{2^n}$$

and probability of success $\geq 1 - \delta$, where $\delta$ is the error tolerance.

### Results

In this work, we used the noise model that represents simplest type of noise processes in a single qubit. The QSVT and non-QSVT algorithms are compared for the bit flip, phase flip, bit-phase flip, and the depolarizing noise channel. The evolution of the state under the noisy channel can be characterized as,

$$\varepsilon(\hat{\rho}) = \sum_{k=1} \hat{E}_k \hat{\rho} \hat{E}_k^\dagger , \tag{7}$$
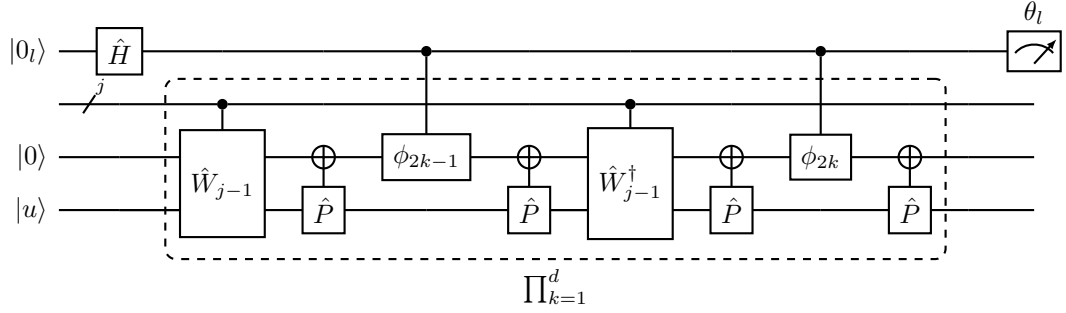
**Figure 2.** The $l^{th}$ section of the QSVT quantum circuit for phase estimation algorithm, where $\phi$ is a phase rotation gate which takes the rotation parameters as argument and the $C_{\hat{P}}NOT$ and $C_{\hat{P}'}NOT$ gates target the ancilla qubit. The expanded form of the $\hat{W}_j$ can be found in[7].

where the operators $\hat{E}_k$ depend on the channel such that $\sum \hat{E}_k^\dagger \hat{E}_k = \hat{I}$. These operators for the chosen noise models are provided in Table 1.

| | | |
|---|---|---|
| Depolarizing | $\sqrt{1-3p/4}\hat{I}$ | $\sqrt{p/4}\hat{\sigma}_i$ |
| Bit Flip | $\sqrt{p}\hat{I}$ | $\sqrt{1-p}\hat{X}$ |
| Phase Flip | $\sqrt{p}\hat{I}$ | $\sqrt{1-p}\hat{Z}$ |
| Bit-Phase Flip | $\sqrt{p}\hat{I}$ | $\sqrt{1-p}\hat{Y}$ |

**Table 1.** The operators corresponding to the different noisy channels used for the noise analysis in Eq. (7). For the depolarizing channel the $\hat{\sigma}_i$ signifies that all Pauli gates are used.

For all the numerical results in the paper, the algorithms were decomposed into the form of the single qubit basic gates set $\{\hat{I}, \hat{X}, \hat{SX}, \hat{RZ}, \hat{CX}\}$ before the noise models were introduced into the gates. The noise was added to all instances of the single qubit gates and the algorithms simulated for a standard of $10,000$ shots and measured in the computational basis as a function of the probability of error $p$[19].

### Grover Search Algorithm

The probability of success for the Grover search algorithm shows the probability of finding the desired state $|m\rangle$. The plots of probability of success found by running the algorithms for $10,000$ shots at each value of $p$ are given in Fig. 3. The figure show that the QSVT Grover search algorithm performs worse than the non-QSVT algorithm for the number of working qubits $n = \{3, 4\}$. The QSVT implementation is such that the Phase Oracle and Diffuser for the non-QSVT algorithm are equivalent to the $C_{\hat{P}}NOT_\phi$ and $V^\dagger C_{\hat{P}'}NOT_\phi V$ shown as blocks in Fig. 1. Hence we can directly compare the noise relation of the QSVT and non-QSVT Grover oracle. A comparison of QSVT and non-QSVT results that QSVT probability of success approaches $1/n$ faster than the non-QSVT results for both values of $n$. The approach to $1/n$ is because of the noise driving the output state to the maximally mixed state. Furthermore, the scan of all results show that the approach is approximately exponential. The faster approach to maximally mixed state for the QSVT algorithm is due to a higher number of gates than the non-QSVT algorithm for the same number of working qubits, as can be seen from Table 2.

| | Non-QSVT | | QSVT | |
|---|---|---|---|---|
| n | No. of Gates | Depth | No. of Gates | Depth |
| 2 | 41 | 28 | 155 | 119 |
| 3 | 82 | 58 | 454 | 367 |
| 4 | 392 | 297 | 1647 | 1328 |
| 5 | 1185 | 927 | 4184 | 3403 |

**Table 2.** Number of gates and depth of the circuit for non-QSVT and QSVT Grover algorithms.

The Grover algorithm essentially rotates the state in a space spanned by the desired output state and the state orthogonal to it. Therefore, the output is a periodic function of the number of iterations. So, it is ideal to see the impact of the number
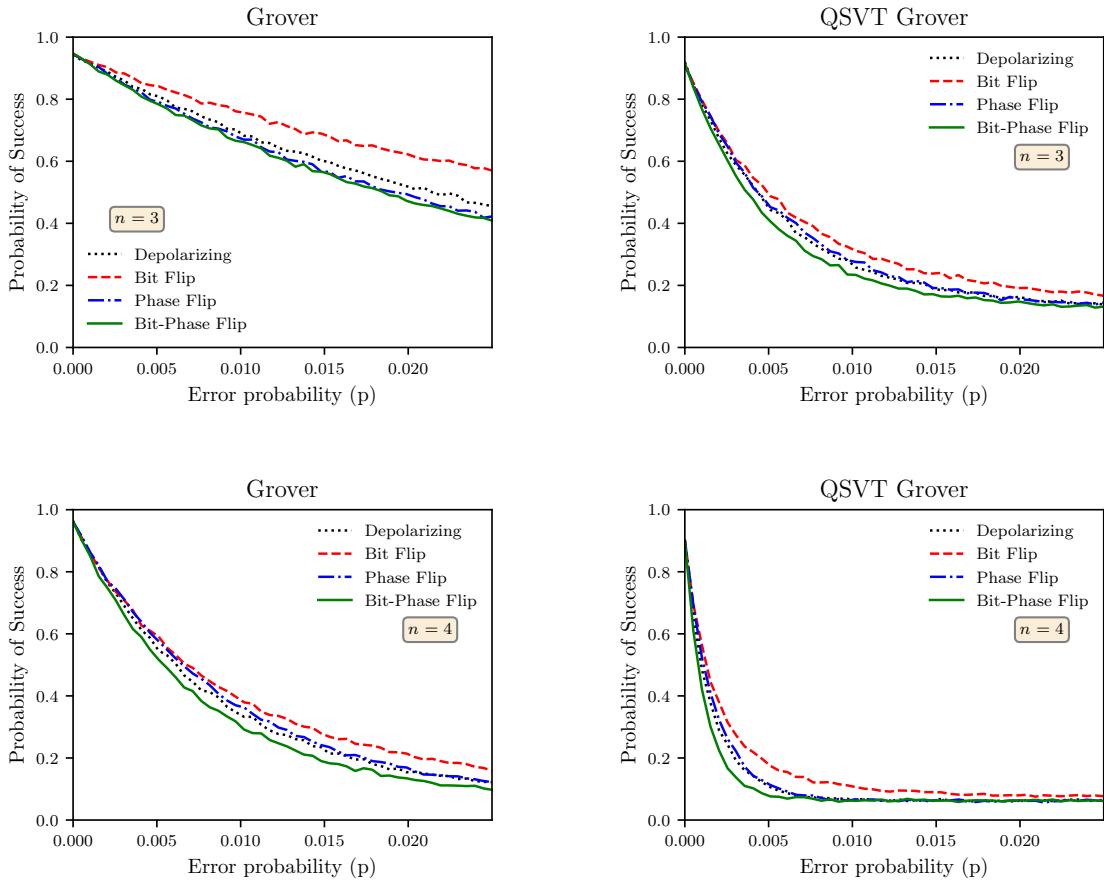
**Figure 3.** The probability of success for various noise models for Non-QSVT and QSVT Grover search algorithms when the number of working qubits were either 3 or 4. The probability of success was computed by running the algorithm for 10,000 shots at each value of $p$.
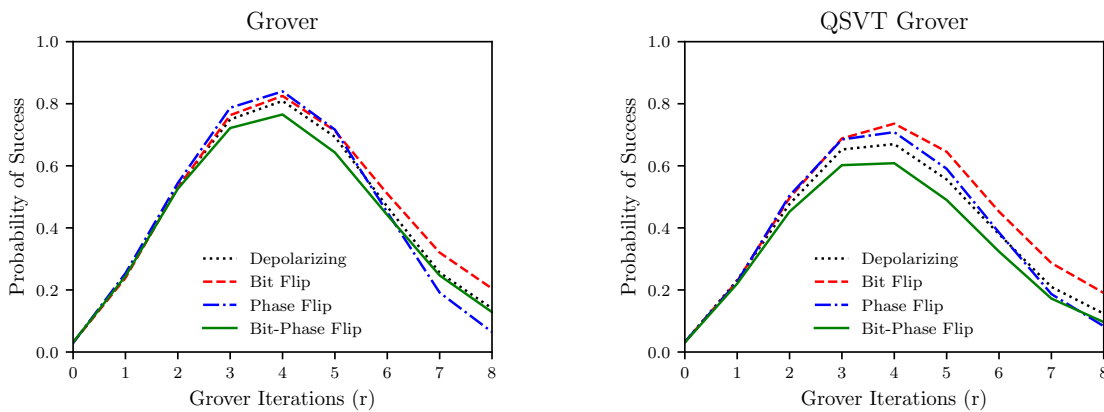


**Figure 4.** Probability of success against the number of iterations of the Non-QSVT and QSVT Grover oracle for different noise channels with fixed probability of error $p = 0.0005$.

of iterations. To see the error accumulation as a function of number of iteration, the probability of success is plotted as a function of number of iteration $r$ in Fig. 4 for $n = 5$ and probability of error $p = 0.0005$. For the search problem of finding one

marked state with $n = 5$, the optimum number of iterations of the Grover oracle is 4. The figure shows that the probability of success for each channel peaks at $r = 4$ and then decrease, though the probability of success is adversely impacted by QSVT implementation of the Grover algorithm.

### Phase Estimation Algorithm

For the comparative noise analysis of the phase estimation algorithm, we have used the average value of the measured phase $\theta'$ when the actual phase $\theta$ was introduced by using the unitary $\hat{U}$. The difference between the measure and actual phase $\theta$ is due to the finite number of working qubits $n$ for the noiseless quantum computer. The main metric to understand the impact of noise is, therefore, the average value of $\theta'$ and its deviation from the actual value of $\theta$.
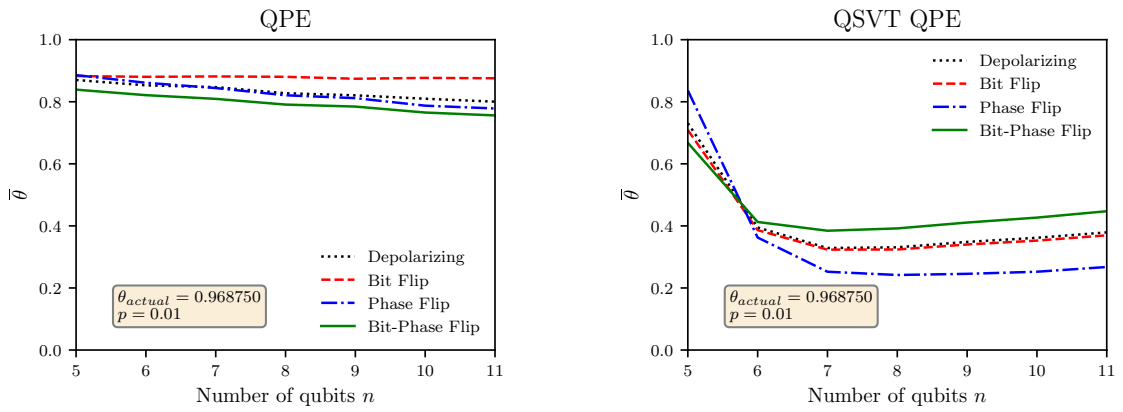


**Figure 5.** Average value of $\theta'$ against the number of working qubits $n$ with probability of error $p = 0.01$ for non-QSVT and QSVT QPE algorithms.

The average value of $\theta'$ for the QSVT and non-QSVT QPE algorithms is shown in Fig. 5 as a function of the number of working qubits. The figure shows that QSVT QPE deteriorate quickly whereas non-QSVT QPE is quite robust to the noise. Actually, it seems that the non-QSVT has almost a linear dependence upon $n$ but QSVT QPE performance decays rapidly.

The impact of noise on the average value of measure $\theta'$ is shown in Fig. 6 as a function of error probability $p$ for a very low and a very high value of phase $\theta$. Similar to the results for the Grover algorithms, the QSVT QPE algorithm has less noise resilience than the non-QSVT algorithm. For low value of $p$, the average value of $\theta'$ is close to the actual value, but eventually approaches $\theta \sim 0.5$ when $p$ increases because the output state approaches the maximally mixed state. However, the approach to the maximally mixed state is very rapid for the QSVT than the non-QSVT implementation of the QPE.

| n | Non-QSVT | | QSVT | |
| --- | --- | --- | --- | --- |
| | No. of Gates | Depth | No. of Gates | Depth |
| 2 | 35 | 23 | 130 | 100 |
| 3 | 52 | 35 | 230 | 175 |
| 4 | 79 | 46 | 350 | 264 |
| 5 | 105 | 57 | 479 | 364 |

**Table 3.** Number of gates for non-QSVT and QSVT QPE algorithms.

Like the Grover search algorithm, the noise dependence of the QSVT and non-QSVT QPE algorithm can be explained by the gate counts used for a $n$ size problem. For the same $n$, the QSVT uses a much larger number of gates, as shown in Table 3. This results in stronger dependence of QSVT implementation on the error probability $p$.

## Discussion

We simulated the implementation of Grover search and quantum phase estimation (QPE) algorithms using original and quantum singular value transformation (QSVT) algorithm for a small number of working qubits relevant to noisy quantum computers. The probability of success for Grover and the average of the measure phase for QPE showed stronger dependence upon the
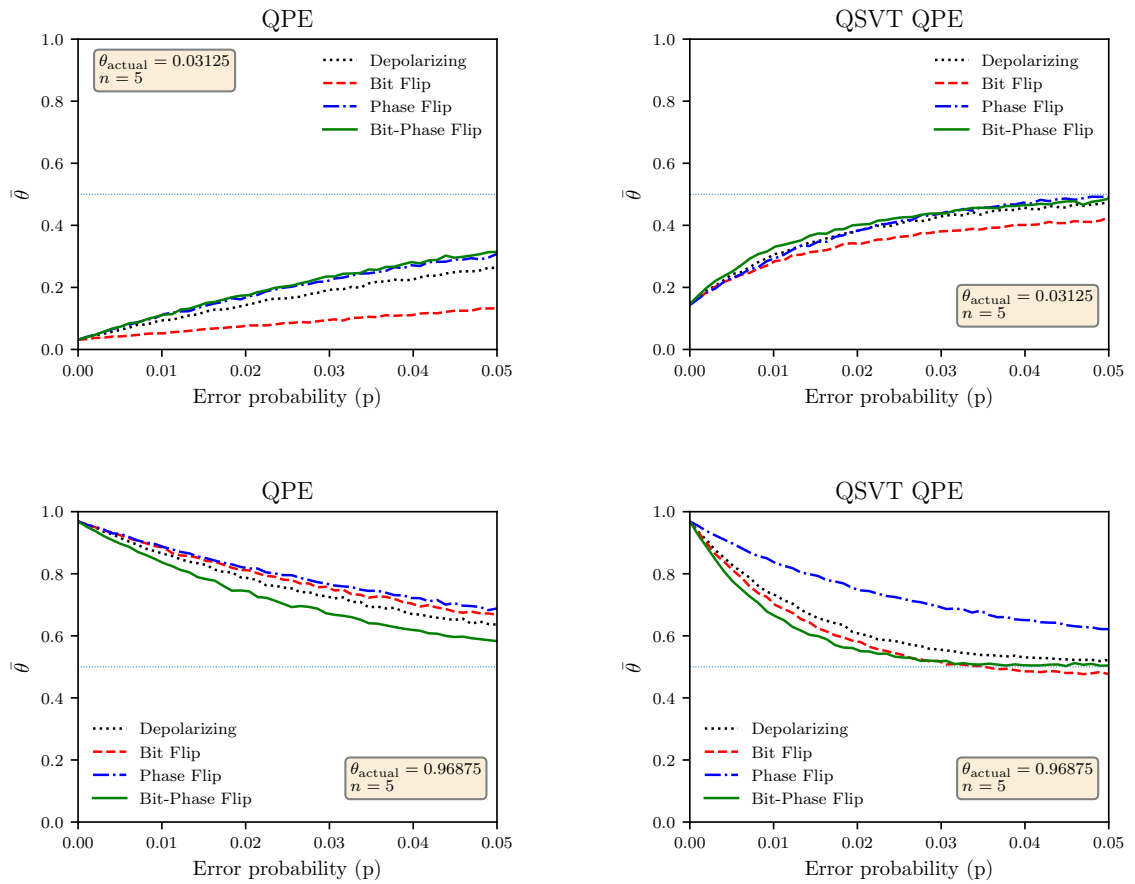
**Figure 6.** Average value of $\theta'$ against the probability of error $p$, for Non-QSVT and QSVT QPE algorithm for two values of $\theta$. The dotted line shows the result when the algorithm has evolved the system to a maximally mixed state.

error probability for QSVT implementation than the original algorithm. This is because of the larger overhead of the number of gates due to the polynomial approximation used in QSVT implementation.

The consistently worse performance for QSVT implementation for four different types of noise models show that the advantage of QSVT algorithm is limited on noisy quantum computers of today[10].

## References

1. Nielsen, M. A. & Chuang, I. L. *Quantum computation and quantum information* (Cambridge university press, 2010).

2. Gilyén, A. *Quantum singular value transformation & its algorithmic applications*. Ph.D. thesis, University of Amsterdam (2019).

3. Low, G. H. & Chuang, I. L. Optimal hamiltonian simulation by quantum signal processing. *Phys. Rev. Lett.* **118**, 010501, DOI: 10.1103/PhysRevLett.118.010501 (2017).

4. Low, G. H. *Quantum signal processing by single-qubit dynamics*. Ph.D. thesis, Massachusetts Institute of Technology (2017).

5. Low, G. H. & Chuang, I. L. Hamiltonian simulation by qubitization. *Quantum* **3**, 163 (2019).

6. Gilyén, A., Su, Y., Low, G. H. & Wiebe, N. Quantum singular value transformation and beyond: exponential improvements for quantum matrix arithmetics. In *Proceedings of the 51st Annual ACM SIGACT Symposium on Theory of Computing*, 193–204 (2019).

7. Martyn, J. M., Rossi, Z. M., Tan, A. K. & Chuang, I. L. Grand unification of quantum algorithms. *PRX Quantum* **2**, 040203, DOI: 10.1103/PRXQuantum.2.040203 (2021).

8. Low, G. H., Yoder, T. J. & Chuang, I. L. Methodology of resonant equiangular composite quantum gates. *Phys. Rev. X* **6**, 041067, DOI: [10.1103/PhysRevX.6.041067](10.1103/PhysRevX.6.041067) (2016).

9. Haah, J. Product Decomposition of Periodic Functions in Quantum Signal Processing. *Quantum* **3**, 190, DOI: [10.22331/q-2019-10-07-190](10.22331/q-2019-10-07-190) (2019).

10. Preskill, J. Quantum computing in the nisq era and beyond. *Quantum* **2**, 79 (2018).

11. Chao, R., Ding, D., Gilyen, A., Huang, C. & Szegedy, M. Finding angles for quantum signal processing with machine precision (2020). [2003.02831](2003.02831).

12. Harrow, A. W., Hassidim, A. & Lloyd, S. Quantum algorithm for linear systems of equations. *Phys. Rev. Lett.* **103**, 150502, DOI: [10.1103/PhysRevLett.103.150502](10.1103/PhysRevLett.103.150502) (2009).

13. Low, I. C. G., Yoder, T. J. & Chuang, I. L. The methodology of composite quantum gates. *arXiv preprint arXiv:1603.03996* (2016).

14. Yoder, T. J., Low, G. H. & Chuang, I. L. Fixed-point quantum search with an optimal number of queries. *Phys. Rev. Lett.* **113**, 210501, DOI: [10.1103/PhysRevLett.113.210501](10.1103/PhysRevLett.113.210501) (2014).

15. Bartubisgin. Bartubisgin/qsvtinqiskit-2021-europe-hackathon-winning-project-: Search with quantum singular value transformation in qiskit.

16. Rall, P. Faster coherent quantum algorithms for phase, energy, and amplitude estimation. *Quantum* **5**, 566 (2021).

17. Kitaev, A. Y., Shen, A. & Vyalyi, M. N. *Classical and quantum computation*. 47 (American Mathematical Soc., 2002).

18. Kitaev, A. Y. Quantum measurements and the abelian stabilizer problem (1995). [quant-ph/9511026](quant-ph/9511026).

19. Noise models (qiskit.providers.aer.noise)¶ (2021).

20. Faizan, M. *Impact of Noise on Quantum Phase Estimation*. Master's thesis, Lahore University of Management Sciences (2022).

21. Ijaz, M. A. *Noise Analysis of Quantum Singular Value Transformation Algorithm*. Bachelor's thesis, Lahore University of Management Sciences (2023).

## Author contributions statement

## Data availability

All data generated or analysed during this study are included in this published article.

# Quanifying magic (and its relation to entanglement) beyond qubits: the case of S=1 chains

**M.Frau,**[1] **P.S.Tarabunga,**[1,2,3] **E. Tirrito,**[2,4] **M. Collura,**[1,3] **and M.Dalmonte**[1,2],

[1]*International School for Advanced Studies (SISSA), 34136 Trieste, Italy*
[2] *The Abdus Salam International Centre for Theoretical Physics (ICTP), Strada Costiera 11, 34151 Trieste, Italy*
[3] *INFN, Sezione di Trieste, Via Valerio 2, 34127 Trieste, Italy*
[4] *Pitaevskii BEC Center, CNR-INO and Dipartimento di Fisica, Universita di Trento, Via Sommarive 14, Trento, I-38123, Italy*

Nonstabilizerness, also known as magic, is a fundamental resource in quantum computing, as it is required to outperform classical simulations. However, there is presently not much understanding on how nonstabilizerness works beyond qubits.

We study magic in different groundstates of a spin 1 Heisenberg chain with uniaxial single ion-type anisotropy. In particular, we exploit a Matrix Product State (MPS) based algorithm to perform Pefect Pauli Sampling of many-body states to estimate some recently introduced measures of magic: the Stabilizer Rényi Entropies (SREs).

We qualitatively show that the $n = 1$ SRE displays dependence from topology, as it is maximum in the topological phase, corroborating the hypothesis of a connection between magic and many-body phenomena. Moreover, we study the scaling of magic with the bond dimension $\chi$ of the MPS. We show that SRE is more stable under truncation compared to entanglement entropy and that it scales as a power law in $\frac{1}{\chi}$.

# Towards microwave experiments in III-V 2DEGs

**R. Gharibaan [1] , P. Viswanathan [1] , and Srijit Goswami [1]**

[1] *QuTech and Kavli Institute of Nanoscience, Delft University of Technology, Delft, 2600 GA, The Netherlands.*

Two-dimensional electron gases (2DEGs) in III-V materials offer a versatile and flexible platform to study hybrid superconductor-semiconductor devices. Recently such 2DEGs have been used to create gate-tunable superconducting qubits and are a promising platform to explore topological systems. In order to study these systems it is desirable to control them at short timescales. However, in general, these 2DEGs are not ideal for microwave frequency experiments, since they significantly lower the quality factor of on-chip microwave resonators due to dielectric losses [1, 2]. This limits the ability to perform fast operations and to study these hybrid systems on short timescales. Moreover, the additional fabrication steps required to create the microwave circuitry are often incompatible with the processing of hybrid devices in the 2DEGs.

These issues can be resolved by utilizing a flip-chip architecture, allowing the microwave resonators and the qubits to have their own separate substrates. This technology will open the path towards higher qubit lifetimes and microwave experiments in III-V 2DEG substrates. My poster includes the current progress in flip-chip fabrication, challenges in fabrication, recent measurements of galvanic connections between chips via indium bumps, research in electrochemical deposition of indium, and future experiments measuring resonator quality factor in flip-chip architecture.

[1] M. Hinderling, D. Sabonis, S. Paredes, D. Haxell, M. Coraiola, S. Kate, E. Cheah, F. Krizek, R. Schott,  W. Wegscheider, F. Nichele, Phys. Rev. Appl., **19**, 054026. (2023).
[2] L. Casparis, M.R. Connolly, M. Kjaergaard, N.J. Pearson, A. Kringhoj, T.W. Larsen, F. Kuemmeth, T. Wang, C. Thomas, S. Gronin, G.C. Gardner, M.J. Manfra, C.M. Marcus, K.D. Petersson, Nature Nanotech **13**, 915–919 (2018).

# Experimental quantum computational chemistry with optimised unitary coupled cluster ansatz

**Shaojun Guo** [1,2,3,*], **Jinzhao Sun** [4,5,*], **Haoran Qian** [1,2,3,*], **Ming Gong** [1,2,3,*], **Yukun Zhang** [4,6], **Fusheng Chen** [1,2,3], **Yangsen Ye** [1,2,3], **Yulin Wu** [1,2,3], **Sirui Cao** [1,2,3], **Kun Liu** [4], **Chen Zha** [1,2,3], **Chong Ying** [1,2,3], **Qingling Zhu** [1,2,3], **He-Liang Huang** [1,2,3], **Youwei Zhao** [1,2,3], **Shaowei Li** [1,2,3], **Shiyu Wang** [1,2,3], **Jiale Yu** [1,2,3], **Daojin Fan** [1,2,3], **Dachao Wu** [1,2,3], **Hong Su** [1,2,3], **Hui Deng** [1,2,3], **Hao Rong** [1,2,3], **Yuan Li** [1,2,3], **Kaili Zhang** [1,2,3], **Tung-Hsun Chung** [1,2,3], **Futian Liang** [1,2,3], **Jin Lin** [1,2,3], **Yu Xu** [1,2,3], **Lihua Sun** [1,2,3], **Cheng Guo** [1,2,3], **Na Li** [1,2,3], **Yong-Heng Huo** [1,2,3], **Cheng-Zhi Peng** [1,2,3], **Chao-Yang Lu** [1,2,3], **Xiao Yuan** [4,6], **Xiaobo Zhu** [1,2,3], and **Jian-Wei Pan** [1,2,3]

[1]*Hefei National Research Center for Physical Sciences at the Microscale and School of Physical Sciences, University of Science and Technology of China, Hefei 230026, China*
[2]*Shanghai Research Center for Quantum Science and CAS Center for Excellence in Quantum Information and Quantum Physics, University of Science and Technology of China, Shanghai 201315, China*
[3]*Hefei National Laboratory, University of Science and Technology of China, Hefei 230088, China*
[4]*Center on Frontiers of Computing Studies, Peking University, Beijing 100871, China*
[5]*Clarendon Laboratory, University of Oxford, Parks Road, Oxford OX1 3PU, United Kingdom*
[6]*School of Computer Science, Peking University, Beijing 100871, China*

Simulation of quantum chemistry is one of the most promising applications of quantum computing. While recent experimental works have demonstrated the potential of solving electronic structures with variational quantum eigensolver (VQE), the implementations are either restricted to nonscalable (hardware efficient) or classically simulable (Hartree-Fock) ansatz, or limited to a few qubits with large errors for the more accurate unitary coupled cluster (UCC) ansatz. Here, integrating experimental and theoretical advancements of improved operations and dedicated algorithm optimisations, we demonstrate an implementation of VQE with UCC for H2, LiH, F2 from 4 to 12 qubits. Combining error mitigation, we produce high-precision results of the ground-state energy with error suppression by around two orders of magnitude. For the first time, we achieve chemical accuracy for H2 at all bond distances and LiH at small bond distances in the experiment. Our work demonstrates a feasible path towards a scalable solution to electronic structure calculation, validating the key technological features and identifying future challenges for this goal.

[*] These authors contributed equally to this work.

Abstract for Conference on New Frontiers in Scaling Quantum: from Materials and Hardware to Architectures and Components (smr 3916)

## Skyrmion-Based Magnetic Recording and Storage

**Yong Hu**

*Department of Physics, College of Sciences, Northeastern University, Shenyang 110819, P. R. China*

Magnetic skyrmions are nanoscale spin configurations that hold promise as information carriers in ultradense memory and logic devices owing to the extremely low spin-polarized currents needed to move them. Although an electrical manipulation of skyrmions has been realized via spin-polarized current based on spin-transfer torque or spin-orbit torque effect, this scheme is energy consuming and may produce massive Joule heating. To reduce energy dissipation and risk of heightened temperatures of skyrmion-based devices, electric field instead of current as stimulus to trigger skyrmion creation/switch is developed. We fabricated a ferromagnetic/ferroelectric [Pt/Co/Ta]$_n$/PMN-PT multiferroic heterostructure, and achieved a non-volatile manipulation of skyrmion switch via magnetoelectric coupling. Our results open a direction for constructing low-energy-dissipation, non-volatile, and multistate skyrmion-based spintronic devices.
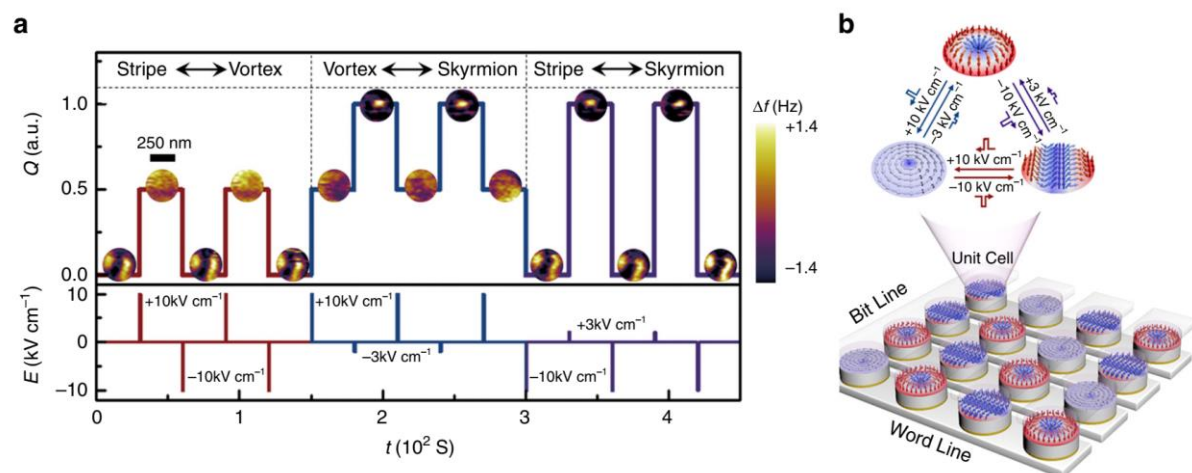
**Fig. 1.** Switching of individual skyrmions induced by pulse electric field.

Furthermore, magnetic skyrmions emerge when the energy of ferromagnetic exchange interaction promoting parallel alignment of spins enters in competition with energies favouring noncollinear alignment of spins such as Dzyaloshinskii-Moriya interaction (DMI), long-range dipole-dipole interaction (DDI), or higher order exchange interaction. We performed an unbiased Monte-Carlo simulation to decipher the roles of diverse energies on the manipulation of skyrmions.

[1] Y. Wang, *et al*., Nat. Commun. **11**, 3577 (2020).
[2] M. X. Sui, Y. Hu, Rare Met. **41**, 3160 (2022).

# Quantum Circuit Optimization based on mid-circuit Entanglement

**Kevin J. Joven** [1]

[1]*Universidad del Valle, Cali-Colombia*

In the field of superconducting quantum processors, where connectivity is often constrained to a limited number of local couplers (e.g. star transmons with up to 7 local couplers [1] or common transmons with up to 4 couplers [2]), addressing these limitations becomes crucial in the NISQ (Noisy Intermediate-Scale Quantum) era. Given the inherent fragility of quantum entanglement, extending the decoherence time by enabling hardware interconnections among neighboring qubits is crucial. In this study, we investigate the impact of entanglement on quantum architecture performance, highlighting how such an approach can enhance the overall efficiency of quantum circuits and QEC codes.

[1] Koch, J., Yu, T. M., Gambetta, J., Houck, A. A., Schuster, D. I., Majer, J., Blais, A., Devoret, M. H., Girvin, S. M., & Schoelkopf, R. J. (2007). Charge-insensitive qubit design derived from the Cooper pair box. *Phys. Rev. A, 76*(4)

[2] R. Versluis, et al. Scalable Quantum Circuit and Control for a Superconducting Surface Code. Phys. Rev. Applied 8, 034021 (2017).

# Exploring fluxon tunneling dynamics in the IST qubit

Lucky N. Kapoor[1], Farid Hassani[1], Alesya Sokolova[1], Igor V. Rozhansky[2], Alexander N. Poddubny[3] and Johannes M. Fink[1]

[1]*Institute of Science and Technology Austria, Klosterneuburg 3400, Austria*
[2]*National Graphene Institute, University of Manchester, Manchester M13 9PL, United Kingdom*
[3]*Weizmann Institute of Science, Rehovot 7610001, Israel.*

In a heavy fluxonium, the wave functions of fluxons become increasingly disjoint as the barrier height between the two potential wells is raised by increasing the Josephson energy. In the IST qubit limit[1], this suppression of fluxon transitions can lead to remarkable relaxation times measured to be on the order of several hours. In this work, we delve into the dynamics of fluxon tunneling and initialization studied in such an IST qubit. We induce inter-well transitions in the qubit by populating the cavity with a large number of photons. Our semi-classical model accurately replicates the tunneling dynamics, encompassing both photon-assisted and non-resonant tunneling between plasmon levels in the two fluxon wells. This model suggests that, at specific values of external flux through the rf-SQUID loop, direct transitions between the wells might become feasible. Furthermore, photon-assisted tunneling enables precise fluxon state preparation, allowing a deeper investigation into tunneling rates. In the future, fast tuning of the barrier, through fast flux control of the Josephson energy, could offer further insights into the tunneling dynamics while also enabling full qubit control of decay-protected fluxon states

[1]  Hassani, Farid, et al. Nature Communications 14.1 (2023): 3968.

# High-impedance resonators based on granular aluminum

**Mahya Khorramshahi** [1], **Martin Spiecker**[1], **Patrick Paluch** [1], **Ritika Dhundhwal** [1], **Nicolas Zapata**[1], **Ioan M. Pop**[1] and **Thomas Reisinger** [1]

[1]*Karlsruhe Institute of Technology, Karlsruhe, Germany*

High-impedance resonators in superconducting quantum circuits are important in the advancement of quantum computing technologies. In particular, impedances surpassing the resistance quantum make it possible to build better-protected qubits and allow for stronger coupling to small-dipole-moment systems with exciting prospects for interfacing to spin qubits or donor spins. Using granular aluminum (GrAl), we've developed compact resonators that work in the low GHz range, with impedances up to 80 kOhm. We characterized the resonators, with GrAl resistivity increasingly close to the superconducting to insulating transition, and report on single photon quality factors, non-linearity, and noise-spectral density.

# Near-power-law temperature dependence of the superfluid stiffness in strongly disordered superconductors

Poor man's scaling and Lie algebras

# Effect of superconductivity on non-uniform magnetization in dirty SF junctions

**Andrei Levin**[1]**, Pavel Ostrovsky**[2]

[1]*University of Ljubljana, Slovenia*
[2] *Karlsruhe Institute of Technology (KIT), Germany*

We consider a junction between a bulk superconductor and a thin ferromagnetic layer on its surface (SF junction) with nonuniform magnetization. In the absence of the superconductor, the most energetically favorable state of the ferromagnet is uniform. On the other hand, Cooper pairs from the superconductor can more efficiently diffuse into the ferromagnet if its magnetization changes in space rapidly enough [1, 2]. We demonstrate that the competition between these two effects leads to the second order phase transition between uniformly magnetized and helical states of the ferromagnet.

We assume the junction is in the dirty limit ($\Delta\tau \ll 1$) and the ferromagnetic layer is sufficiently thin ($d \ll \sqrt{D/\{\Delta, h\}}$). In addition, we also assume a tunnel boundary between the superconductor and the ferromagnet. These assumptions allow us to describe the hybrid system in the framework of the 2D Usadel equation.

We have minimized the free energy of the system allowing for an arbitrary nonuniform magnetic state and constructed a Landau functional expanding the free energy in powers of magnetization gradients. This calculation establishes conditions for the phase transition between uniform and helical magnetic states. In particular, we have observed a quite unexpected "resonance" phenomenon: when the exchange energy of the ferromagnet equals the proximity-induced superconducting order parameter, transition to the helical state occurs irrespective of the value of ferromagnetic stiffness.

In addition to describing the phase transition, our method also allows exploring a general case of arbitrary system parameters. In particular, we can determine the magnitude of the helical state wave vector far from the phase transition. This will be the subject of our future studies.

[1] F. S. Bergeret, K. B. Efetov, A. I. Larkin, Phys. Rev. B **62**, 11872 (2000).
[2] F. S. Bergeret, A. F. Volkov, and K. B. Efetov, Rev. Mod. Phys. **77**, 1321 (2005).

# The butterfly effect in a Sachdev-Ye-Kitaev quantum dot system

We study the out-of-time-order correlation function (OTOC) in a lattice extension of the Sachdev-Ye-Kitaev (SYK) model with quadratic perturbations. The results obtained are valid for arbitrary time scales, both shorter and longer than the Ehrenfest time. We demonstrate that the region of well-developed chaos is separated from the weakly chaotic region by the "front region", which moves ballistically across the lattice. Front velocity is calculated for various system's parameters, for the first time for SYK-like models.

# Anomalous Josephson effect in superconducting multilayers

A. S. Osin,[1] Alex Levchenko,[2] and Maxim Khodas[1]

[1]*Racah Institute of Physics, Hebrew University of Jerusalem, Jerusalem 91904, Israel*
[2]*Department of Physics, University of Wisconsin–Madison, Madison, Wisconsin 53706, USA*
(Dated: October 21, 2023)

We investigate the Josephson current-phase relation in a planar diffuse tunnelling superconducting multilayer junction in the parallel magnetic field. We compute the supercurrent for a fixed jump of the phase of the order parameter at each of the two insulating interfaces. This allows us to find the current-phase relation of the junction. The perturbation theory in junction conductance allows us to determine the first and second harmonics of the current-phase relation at a given magnetic field. Strong spin-orbit interaction in $S'$-region makes the Josephson effect anomalous. Specifically, the combination of the spin-orbit and Zeeman interactions give rise to an effective vector potential. This causes each harmonic of the current-phase relation to shift without changing the overall shape of the current-phase relation.

P20

# Theory of free fermions under random projective measurements

**Igor Poboiko**[1,2], **Paul Pöpperl**[1,2]**, Igor Gornyi**[1,2]**, Alexander Mirlin**[1,2]

[1]*Institute for Quantum Materials and Technologies, Karlsruhe Institute of Technology*
[2]*Institut für Theorie der Kondensierten Materie, Karlsruhe Institute of Technology*

We develop a theory of measurement-induced phase transitions (MIPT) for *d*-dimensional lattice free fermions subject to random projective measurements of local site occupation numbers. Our analytical approach is based on the Keldysh path-integral formalism and replica trick.

In the limit of rare measurements, $\gamma \ll J$ (where $\gamma$ is measurement rate per site and $J$ is hopping constant), we derive a non-linear sigma model (NLSM) as an effective field theory of the problem. Its replica-symmetric sector is a $\mathrm{U}(2)/\mathrm{U}(1){\times}\mathrm{U}(1)$ NLSM describing diffusive behavior of average density fluctuations. The replica-asymmetric sector, which describes propagation of quantum information in a system, is a $(d{+}1)$-dimensional isotropic NLSM defined on $\mathrm{SU}(\mathrm{R})$ manifold with the replica limit $R \to 1$, establishing close relation between MIPT and Anderson transitions. On the Gaussian level, valid in the limit $\gamma/J \to 0$, this model predicts "critical" (i.e. logarithmic enhancement of area law) behavior for the entanglement entropy.

However, one-loop renormalization group analysis shows [1] that for $d{=}1$, the logarithmic growth saturates at a finite value $\sim(J/\gamma)^2$ even for rare measurements, implying existence of a single area-law phase. The crossover between logarithmic growth and saturation, however, happens at an exponentially large scale, $\ln(l_{corr}){\sim}J/\gamma$, thus making it easy to confuse with a transition in a finite-size system.
Furthermore, utilizing $\varepsilon$-expansion, we demonstrate [2] that the "critical" phase is stabilized for $d > 1$ with a transition to the area-law phase at a finite value of $\gamma/J$.

The analytical calculations are supported and are in excellent agreement with extensive numerical simulations [1,2] for $d{=}1$ and $d{=}2$. For $d{=}2$ we determine numerically the position of the transition and estimate the value of correlation length critical exponent.

[1] I.P., P. Pöpperl, I. Gornyi, A.D. Mirlin, https://arxiv.org/abs/2304.03138 (accepted to Phys. Rev. X)
[2] I.P., I. Gornyi, A.D. Mirlin https://arxiv.org/abs/2309.12405

# Quantum error correction beyond the toric code

**Garima Rajpoot** [1] **, Komal Kumari** [1,2] **, and Sudhir R. Jain** [1,2,3]

[1](Garima Rajpoot) *Bhabha Atomic Research Centre, Mumbai-400085, INDIA*
[2] *Homi Bhabha National Institute, Training School Complex, Anushaktinagar, Mumbai-400094, INDIA*
[3]*UM-DAE Centre for Excellence in Basic Sciences, University of Mumbai, Vidyanagari Campus, Mumbai-400098, INDIA*

We construct surface codes corresponding to genus greater than one in the context of quantum error correction. The architecture is inspired by the topology of invariant integral surfaces of certain non-integrable classical billiards. Corresponding to the fundamental domains of rhombus and square torus billiard, surface codes of genus two and five are presented here. There is significant improvement in encoding rates and code distance, in addition to immunity against noise.

# Intensity statistics inside an open wave-chaotic cavity with broken time-reversal invariance

**Elizaveta Safonova**[1] **and Yan Fyodorov**[2]

[1] *University of Ljubljana, Ljubljana 1000, Slovenia*
[2]*King's College London, Department of Mathematics, London WC2R 2LS, United Kingdom*

Using the supersymmetric method of random matrix theory within the Heidelberg approach framework we provide statistical description of stationary intensity sampled in locations inside an open wave-chaotic cavity, assuming that the time-reversal invariance inside the cavity is fully broken. In particular, we show that when incoming waves are fed via a finite number $M$ of open channels the probability density $\mathcal{P}(I)$ for the single-point intensity $I$ decays as a powerlaw for large intensities: $\mathcal{P}(I) \sim I^{-(M+2)}$, provided there is no internal losses. This behaviour is in marked difference with the Rayleigh law $\mathcal{P}(I) \sim \exp(-I/\overline{I})$ which turns out to be valid only in the limit $M \to \infty$. We also find the joint probability density of intensities $I_1, \ldots, I_L$ in $L > 1$ observation points, and then extract the corresponding statistics for the maximal intensity in the observation pattern. For $L \to \infty$ the resulting limiting extreme value statistics (EVS) turns out to be different from the classical EVS distributions.

# Two-way quantum teleportation under correlated noise

**C. Seida**[1,2], **A. El Allati**[2], and **Y. Hassouni**[1]

[1](*Presenting author underlined*) *ESMaR, faculty of sciences Mohammed V university of Rabat*
[2] *Laboratory of RD in Engineering Sciences, Faculty of Sciences and Techniques Al-Hoceima,*
*Abdelmalek Essaadi University, Tetouan, Morocco*

In this poster, we investigate bidirectional quantum teleportation of quantum states, for the case in which qubits from the quantum channel of teleportation are distributed by typical correlated noisy channels such as bit-flip, phase-flip, depolarizing, and amplitude damping channels. Expressions of the fidelities of teleportation, and quantum Fisher information are evaluated, we found that all these quantities depend on factor noise and the correlation strength of the noisy channel. It is shown that the effect of the noise on the fidelities of teleportation, and on quantum Fisher information could be noticeably reduced due to the existence of the noise channel correlations.

[1] C. Seida, A. El Allati, N. Metwally, Y. Hassouni, (2021). The Eur Phys J D, **75**(6), 170 (2021).
[2] Y. L. ALi, C. H. Liao, L. Yao, X. Xiao, Res in Phy, **107010** (2023).
[3] C. Seida, A. El Allati, N. Metwally, Y. Hassouni, Mod Phys Lett A, **35**(33), 2050272 (2020).

# Fast-forward generation of non-equilibrium steady states of a charged particle under the magnetic field

Iwan Setiawan[1], Ryan Sugihakim[2], Bobby Eka Gunara[2], Shumpei Masuda[3], Katsuhiro Nakamura[4]

[1]Department of Physics Education, University of Bengkulu, Kandang Limun, Bengkulu 38371, Indonesia,
[2]Theoretical High Energy Physics, Institut Teknologi Bandung, Jalan Ganesha 10, Bandung 40132, Indonesia,
[3]Research Center for Emerging Computing Technologies (RCECT), National Institute of Advanced Industrial Science and Technology (AIST), 1-1-1, Umezono, Tsukuba, Ibaraki 305-8568, Japan,
[4]Faculty of Physics, National University of Uzbekistan, Vuzgorodok, Tashkent 100174, Uzbekistan

Abstract

The fast-forward (FF) is one of the ideas to speed up the dynamics of given systems, and reproduces series of events on a shortened time scale, just like rapid projection of movie films on a screen. Considering a charged particle under the electromagnetic field, we present a scheme of FF generation of its non-equilibrium steady state, which realizes with complete fidelity the underlying quantum adiabatic dynamics throughout the FF protocol. We then apply the scheme to Landau states of a clean spin-less electron gas in a 2D $x - y$ plane under the constant magnetic field $B$ in the $z$ direction. We have found how the electric field should be applied in rapid preparation of the quantum-mechanical Hall state as a non-equilibrium steady state. The FF electric field expressed in terms of the time-scaling function is found to be common to both the ground and excited Landau states. The FF driving avoids the decoherence inevitable in slow adiabatic procedures and eliminates the undesired mixing among Landau states with different quantum numbers that usually occurs in fast control.

In this scheme, we regularize and fast forward the vector and scalar potentials to guarantee the adiabatic motion, here is the regularization term and fast forward variant (FF) :

$$\tilde{\mathbf{A}} = m\frac{1}{\bar{\phi}_n^2}\int^{\mathbf{r}} d\mathbf{r}'\partial_R\bar{\phi}_n^2,$$

$$\tilde{V} = -\hbar\partial_R\eta + \frac{1}{m}\left(\hbar\nabla\eta - \mathbf{A}_0\right)\cdot\tilde{\mathbf{A}}$$

$$= -\hbar\partial_R\eta + \left(\hbar\nabla\eta - \mathbf{A}_0\right)\cdot\frac{1}{\bar{\phi}_n^2}\int^{\mathbf{r}} d\mathbf{r}'\partial_R\bar{\phi}_n^2.$$

$$\mathbf{A}_{FF} = \mathbf{A}_0 + v(t)\tilde{\mathbf{A}}$$

$$= \mathbf{A}_0 + mv(t)\frac{1}{\bar{\phi}_n^2}\int^{\mathbf{r}} d\mathbf{r}'\partial_R\bar{\phi}_n^2,$$

$$V_{FF} = V_0 + v(t)\tilde{V} - \frac{v(t)^2}{2m}\tilde{\mathbf{A}}^2$$

$$= V_0 - v(t)\hbar\partial_R\eta + \frac{v(t)}{m}(\hbar\nabla\eta - \mathbf{A}_0)\cdot\tilde{\mathbf{A}} - \frac{v(t)^2}{2m}\tilde{\mathbf{A}}^2.$$

The application of this scheme to Quantum Mechanical Hall System (QMHS) :

The QMHS is realized in a clean spinless electron gas confined in the $x$ - $y$ plane with the magnetic field $\mathbf{B} = B\mathbf{e}z$ and electric field $\mathbf{E} = E\mathbf{e}x$. Then the current appears in the $y$ direction, $\mathbf{J} = J\mathbf{e}y$, we obtain,

$$\tilde{\mathbf{A}} = (\tilde{A}_x, \tilde{A}_y),$$

$$\tilde{A}_x = m\frac{1}{\bar{\phi}_n^2}\int^x dx'\partial_R\bar{\phi}_n^2 = -m,$$

$$\tilde{A}_y = 0.$$

$$\mathbf{A}_{FF} = \left(-mv(t), (x - \int_0^t v(t')dt')B\right),$$

$$V_{FF} = -\mathcal{E}(x - \int_0^t v(t')dt') - \frac{1}{2}m(v(t))^2.$$

$$\mathbf{B}^{FF} = \nabla\times\mathbf{A}_{FF} = B\mathbf{e}_z,$$

$$\mathbf{E}^{FF} = -\frac{\partial}{\partial t}\mathbf{A}_{FF} - \nabla V_{FF}$$

$$= (\mathcal{E} + m\dot{v}(t), v(t)B).$$
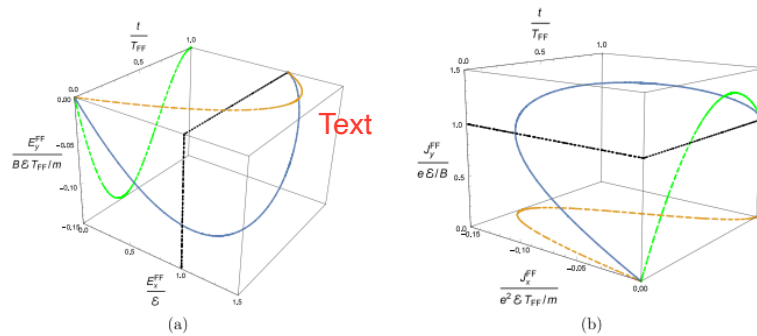


**Fig. 1.** 3D plot of the $x$, $y$ components of the FF electric field and electric current as a function of time $t$: (a) time dependence $E_x^{FF}$, $E_y^{FF}$ (solid curved lines) and its projection onto $E_x^{FF} - t$ and $E_y^{FF} - t$ planes (broken curved lines); (b) time dependence of $J_x^{FF}$, $J_y^{FF}$ (solid curved lines) and its projection onto $J_x^{FF} - t$ and $J_y^{FF} - t$ planes (broken curved lines). The dotted straight lines indicate the value of $E_x^{FF}$ in (a) and that of $J_y^{FF}$ in (b) at the end of the FF protocol.

We have obtained FF vector and scalar potentials, necessary to realize the significant target state of quantum systems at any desired short time

References : Setiawan, et al, Prog. Theor. Exp. Phys. 2023 063A04
Masuda and Nakamura, , Phys. Rev. A 84, 043434

Thanks to PDUPT :
Kemdikbudristek 2023

# Multiplexed control scheme for scalable superconducting quantum processor

**Pan Shi[1,2], and Fei Yan[1]**

[1] *Beijing Academy of Quantum Information Sciences, 100193, Beijing, China*
[2] *School of physics, Wuhan University, 430072, Wuhan, China*

In this research, we present a multiplexed control scheme compatible with state-of-the-art superconducting qubit technologies, addressing critical challenges in large-scale quantum information processing. Our design allows simultaneous precise control of multiple qubits and couplers through shared control lines, markedly reducing wiring complexity, cooling power and space requirements. We also provide variant solutions according the gate type and qubit type. We expect the demand for control lines can be reduced by 1-2 orders of magnitude in the near future, presenting a promising pathway for scaling up quantum processors.

# Many-body magic via Pauli-Markov chains

**Poetri S. Tarabunga** [1,2,3], **Emanuele Tirrito** [1,4], **Titas Chanda** [1,5], and **Marcello Dalmonte** [1,2]

[1]*The Abdus Salam International Centre for Theoretical Physics (ICTP), Strada Costiera 11, 34151, Trieste, Italy*
[2]*SISSA, Via Bonomea 265, 34136, Trieste, Italy*
[3]*INFN, Sezione di Trieste, Via Valerio 2, 34127, Trieste, Italy*
[4]*Pitaevskii BEC Center, CNR-INO and Dipartimento di Fisica, Universita di Trento, Via Sommarive 14, Trento,*
[5]*Department of Physics, Indian Institute of Technology Indore, Khandwa Road, Simrol, Indore, 453552, India*

We introduce a method to measure many-body magic in quantum systems based on a statistical exploration of Pauli strings via Markov chains. We demonstrate that sampling such Pauli-Markov chains gives ample flexibility in terms of partitions where to sample from: in particular, it enables to efficiently extract the magic contained in the correlations between widely-separated subsystems, which characterizes the nonlocality of magic. Our method can be implemented in a variety of situations. We describe an efficient sampling procedure using Tree Tensor Networks, that exploits their hierarchical structure leading to a modest $O(\log N)$ computational scaling with system size. To showcase the applicability and efficiency of our method, we demonstrate the importance of magic in many-body systems via the following discoveries: (a) for one dimensional systems, we show that long-range magic displays strong signatures of conformal quantum criticality (Ising, Potts, and Gaussian), overcoming the limitations of full state magic; (b) in two-dimensional $Z_2$ lattice gauge theories, we provide conclusive evidence that magic is able to identify the confinement-deconfinement transition, and displays critical scaling behavior even at relatively modest volumes. Finally, we discuss an experimental implementation of the method, which only relies on measurements of Pauli observables.

# Quantifying non-stabilizerness through entanglement spectrum flatness

# Optical readout of a superconducting qubit using a piezo-optomechanical transducer

<u>T.C. van Thiel</u>[1], M.J. Weaver[1], F. Berto[1], P. Duivestein[1], M. Lemang[1], K.L. Schuurman[1],
M. Žemlička[1], F. Hijazi[1], A.C. Bernasconi[1], E. Lachman[2], M. Field[2], Y. Mohan[2],
F.K. de Vries[3], C.C. Bultink[3], J. van Oven[3], J.Y. Mutus[2], R. Stockill[1] and S. Gröblacher[1]

[1]*QphoX B.V., Elektronicaweg 10, 2628 XG Delft, The Netherlands*
[2]*Rigetti Computing Inc., 775 Heinz Avenue, Berkeley, California, 94710, United States*
[3]*Qblox B.V., Delftechpark 22, 2628XH, Delft, The Netherlands*

Superconducting quantum processors have made significant progress in size and computing potential. As a result, the practical cryogenic limitations of operating large numbers of superconducting qubits are becoming a bottleneck for further scaling. Due to the low thermal conductivity and the dense optical multiplexing capacity of telecommunications fiber, converting qubit signal processing to the optical domain using microwave-to-optics transduction would significantly relax the strain on cryogenic space and thermal budgets [1]. Here, we demonstrate high-fidelity multi-shot optical readout through an optical fiber of a superconducting transmon qubit connected via a coaxial cable to a fully integrated piezo-optomechanical transducer [2, 3]. Using a demolition readout technique, we achieve a multi-shot readout fidelity of $> 0.99$ at $6\,\mu\mathrm{W}$ of optical power transmitted into the cryostat with as few as 200 averages, without the use of a quantum-limited amplifier. With improved frequency matching between the transducer and the qubit readout resonator, we anticipate that single-shot optical readout is achievable. Due to the small footprint ($< 0.15\,\mathrm{mm}^2$) and the modular fiber-based architecture, this device platform has the potential to scale towards use with thousands of qubits. Our results illustrate the potential of piezo-optomechanical transduction for low-dissipation operation of large quantum processors.

[1] F. Lecocq, F. Quinlan, K. Cicak, J. Aumentado, S. Diddams, and J. Teufel, Nature **591**, 575 (2021).
[2] T.C. van Thiel, M.J. Weaver, F. Berto, P. Duivestein, M. Lemang, K.L. Schuurman et al., arXiv:2310.06026 (2023)
[3] M.J. Weaver, P. Duivestein, A.C. Bernasconi, S. Scharmer, M. Lemang, T.C. van Thiel et al. Nat. Nanotechnology (2023).

# Suppressing spurious transitions using spectrally balanced derivative pulse

**Ruixia Wang** [1] , **Jiayu Ding** [1,2] , **Yang Gao** [1,3] , **Zhikun Han** [1,4] , **Fei Yan** [1] , and **Haifeng Yu** [1]

[1] *Beijing Academy of Quantum Information Sciences, Beijing, China*
[2] *Department of Physics, Nanjing University, Nanjing, China*
[3] *Institute of Physics, Chinese Academy of Sciences, Beijing, China*
[4] *Shenzhen Institute for Quantum Science and Engineering, Southern University of Science and Technology, Shenzhen, Guangdong, China*

In scalable superconducting quantum computing, spurious transitions due to crosstalk degrade the performance of quantum operations. The Derivative Removal by Adiabatic Gate (DRAG) technique has been widely used for eliminating the leakage to non-computational levels during single-qubit gate operations. In this work, we propose and demonstrate a practical pulse-shaping technique extended from DRAG for suppressing spurious transition between qubits in a superconducting quantum processor. Our pulse features balanced spectral shaping which leads to effective blocking of specific transitions. This method can be extended to the case with multiple unwanted couplings among multiple qubits. It can further be used to suppress the loss resulting from the harmful interactions between the qubits and two-level systems or other undesired parasitic couplings to facilitate the realization of scalable quantum computing.

# Logical Magic State Preparation with Fidelity beyond the Distillation Threshold on a Superconducting Quantum Processor

# Near quantum-limited amplification up to 1 T using grAl resonators

**Nicolas Zapata [1], Ivan Takmakov[1], Simon Günzler[1,2], Ameya Nambisan[1], Dennis Rieger[1,2], Wolfgang Wernsdorfer[1,2], and Ioan M Pop[1,2]**

[1]*IQMT (Institute of Quantum Materials and Technologies), KIT (Karslruhe Institute of Technology), Germany*
[2]*PHI (Physikaliches Institut), KIT (Karslruhe Institute of Technology), Germany*

Josephson Junction based amplifiers have become essential components for the readout of microwave quantum circuits. Despite the advances made over the last decade, they still have limited applicability in systems that require high magnetic fields. The use of high kinetic inductance materials like granular Aluminum (grAl), opens the path for low noise amplification in Tesla fields thanks to their in-plane resilience [1] and negligible high order non-linearities [2], which is particularly attractive for the readout of semiconducting spin-qubits [3] and single molecular magnet qubits [4]. Here we present a non-degenerate parametric amplifier made of two coupled grAl resonators forming a Bose-Hubbard dimer [5, 6]. We report near quantum-limited 20 dB amplification, with an instantaneous bandwidth of few MHz and signal-to-pump detuning above 100 MHz, which was stable up to 1 T.

[1] K. Borisov, et al., Appl. Phys. Lett. **117**, 120502 (2020).
[2] N. Maleeva, et al., Nat. Comm. **9**, 3889 (2018).
[3] J. Stehlik, et al., Phys. Rev. Applied. **4**, 014018 (2015).
[4] C. Godfrin, et al., Phys. Rev. Lett. **119**, 187702 (2017).
[5] C. Eichler, et al., Phys. Rev. Lett. **113**, 110502 (2014).
[6] P. Winkel, I. Takmakov, et al., Phys. Rev. Applied. **13**, 024015 (2020).